Preparation and structural characterization of organotin(IV) complexes with ligands containing a hetero {N} atom and a hydroxy group or hydroxy and carboxyl groups

Attila Szorcsik [a], László Nagy [b,*], Michelangelo Scopelliti [c], Andrea Deák [d], Lorenzo Pellerito [c], Kaspar Hegetschweiler [e]

[a] *Bio-inorganic Chemistry Research Group of Hungarian Academy of Sciences, Department of Inorganic and Analytical Chemistry, University of Szeged, H-6701, Szeged, P.O. Box 440, Hungary*
[b] *Department of Inorganic and Analytical Chemistry, University of Szeged, H-6701, Szeged, PO Box 440, Hungary*
[c] *Dipartimento di Chimica Inorganica e Analitica "Stanislao Cannizzaro", Universita di Palermo, Viale delle Scienze, Parco d'Orleans, 90128 Palermo, Italy*
[d] *Institute of Chemistry, Chemical Research Centre of the Hungarian Academy of Sciences, P.O. Box 17, H-1525 Budapest, Hungary*
[e] *Anorganische Chemie, Universitäs des Saarlandes, Postfach 151150, D-66041 Saarbrücken, Germany*

Abstract

Twenty-two *n*-butyltin(IV) and *t*-butyltin(IV) complexes of ligands containing an –OH (–C═O) group or –OH and –COOH groups and an aromatic {N} donor atom were prepared by metathetical reactions. On the basis of the FT-IR and Mössbauer spectroscopic data, molecular structures were assigned to these compounds. The binding sites of the ligands were identified by means of FT-IR spectroscopic measurements, and it was found that in most cases the organotin(IV) moiety reacts with the phenolic form of these ligands. In the complexes with –OH and –COOH functions, the –COOH group is coordinated to the organotin(IV) centres in a monodentate manner. The ^{119}Sn Mössbauer and the FT-IR studies support the formation of trigonal bipyramidal (TBP) and octahedral (O_h) molecular structures. Furthermore, X-ray diffraction analysis has been performed on the *n*-butyltin(IV)- and *t*-butyltin(IV)-8-quinol 8-olato-*O,N* single crystals. The hexacoordinated tin centres exhibit *cis*-octahedral geometry in both complexes.
© 2005 Elsevier B.V. All rights reserved.

Keywords: Organotin(IV); FT-IR; Mössbauer spectroscopy; X-ray diffraction

1. Introduction

Various classes of organotin(IV) compounds exhibit biological (e.g., antitumour) activity [1,2]. Organotin(IV) complexes with ligands containing phenolic –OH or phenolic –OH and –COOH groups and an aromatic {N} donor atom comprise an interesting class of such complexes, but up to now only a few publications have been reported on their molecular structures.

Complexes of $R_nSn(IV)^{(4-n)+}$ (R = alkyl or aryl groups, n = 1 − 3) with 8-hydroxyquinoline and related ligands have been investigated by means of X-ray diffraction [3–6], ^{119}Sn Mössbauer spectroscopy [7–10], IR, NMR, UV–vis and other techniques [11,12]. Huber and co-workers [13] found that the complex *p*-chlorophenyl-tris(8-quinolinato)tin(IV) · 2CHCl$_3$ is monomeric and contains a hepta-coordinated tin atom in a pentagonal-bipyramidal (PBP) environment. In the

* Corresponding author. Tel.: +36 62 544340; fax: +36 62 420505.
E-mail address: laci@chem.u-szeged.hu (L. Nagy).

corresponding monoaryltin(IV) and monobenzyltin(IV) complexes, the ligand is coordinated to the metal centre in a bidentate manner, while in triorganotin(IV) quinolinates its coordination mode is monodentate.

The bifunctional ligands hydroxypyridine, hydroxypyrimidine and hydroxyquinoline contain both a neutral coordinating {N} atom and a negatively charged {O$^-$} coordination site, which can simultaneously be attached to two different metal ions. Such ligands therefore are suitable agents for the synthesis of mixed metal complexes [14]. Maity et al. [15] reported a novel type of mixed dinuclear cyclopalladated complexes of azobenzenes with 2-hydroxypyridine and 2-mercaptopyridine. In these complexes, the phenolic hydroxy moiety is deprotonated, and generally abbreviated as {N,O}. Single-crystal X-ray diffraction analysis revealed that the {N,O}-bridged dimer [Pd(A)(μ-N,O)]$_2$ (where A denotes *ortho*-metallated azobenzene or its derivatives) exhibits a strong Pd$\cdots$Pd interaction. Moreover, 3-hydroxypyridine could be as effective as 2-hydroxypyridine in building oxalate-containing polynuclear metal complexes. In these complexes, the divalent metal centres (Co, Ni) are in distorted octahedral (O$_h$) environment, defined by four oxygen atoms from two symmetry-related bridging oxalato ligands and the pyridine nitrogen atoms from two *cis*-oriented aromatic ligands [16].

The hydroxypyridine-carboxylic acids were found to be bound to different organotin(IV) cations in a variety of ways, i.e., via (i) monodentate, (ii) bridging, (iii) {N,O} or (iv) {O,O} chelating [17,18] coordination modes. They therefore tend to form four-, five- and six-membered chelate rings and to undergo keto-enolic tautomerization (Scheme 1).

It has recently been demonstrated that the reactions of pyridine mono- and dicarboxylato anions with ^{n}Bu$_2$Sn(IV)$^{2+}$ [19] and ^{t}Bu$_2$Sn(IV)$^{2+}$ [20] results in the formation of polynuclear complexes. In these ^{n}Bu$_2$Sn(IV)$^{2+}$ and ^{t}Bu$_2$Sn(IV)$^{2+}$ 2-picolinato and pyridine-2,6-dicarboxylato complexes, the central Sn(IV) ion is hepta- and pentacoordinated in a PBP [19] or square-pyramidal [20] coordination environment. Nevertheless, the literature is sparse on the main group IV elements coordination complexes containing hydroxy-heterocyclic ligands. Therefore, on the basis of our previous experience, a systematically designed series of complexes containing ^{n}Bu$_2$Sn(IV)$^{2+}$ and ^{t}Bu$_2$Sn(IV)$^{2+}$ ions and hydroxypyri-

dine, hydroxypyrimidine, hydroxyquinoline and mono-hydroxy-carboxylate ligands have been prepared. The structural data obtained reveal the influence of the nature and steric positions of the donor atoms on the coordination sphere of the Sn centre. Accordingly, the molecular structures of the complexes were established by FT-IR and Mössbauer spectroscopy. X-ray diffraction analyses of both ^{n}Bu$_2$Sn(IV)$^{2+}$- and ^{t}Bu$_2$Sn(IV)$^{2+}$-8-hydroxyquinolinate, which were obtained in single-crystal form, were also performed.

2. Experimental

2.1. Materials

^{n}Bu$_2$SnCl$_2$ and ^{n}Bu$_2$SnO were purchased from Fluka, and ^{t}Bu$_2$SnCl$_2$ was a Sigma–Aldrich product. 2-Hydroxypyridine {HL^1}, 3-hydroxypyridine {HL^2}, 4-hydroxypyridine {HL^3}, 2,3-dihydroxypyridine {H$_2$L^4}, 4,6-dihydroxypyrimidine {H$_2$L^5}, 8-hydroxyquinoline {HL^6}, 2,4-quinolinediol {H$_2$L^7}, 6-hydroxypicolinic acid {H$_2$L^8}, 3-hydroxypicolinic acid {H$_2$L^9}, 2-hydroxynicotinic acid{H$_2$L^{10}} and 6-hydroxynicotinic acid {H$_2$L^{11}} were from Sigma–Aldrich. All the starting reagents were of A.R. grade and were used without further purification. The chemical formulae of the ligands with the corresponding shorthands used throughout the text are shown in Fig. 1.

2.2. Syntheses

It has been reported [21] that hydroxypyridines undergo tautomerization reactions with pyridones, and the equilibrium of the tautomerization in aqueous solution favours the pyridone isomer for 2- and 4-hydroxypyridine (Scheme 1). This could make the electron-withdrawing effect of the oxygen more pronounced in the coordinated ligand and thus could further stabilize the back-bonding effect. In basic solution, this tautomerization is less favourable. The tautomerization of 3-hydroxypyridine to its pyridone form is less favoured than in 2- and 4-hydroxypyridine, and therefore the electron-withdrawing effect of the hydroxy group is insignificant. Accordingly, in the case of 3-hydroxypyridine, only the hydroxy isomers are able to form stable complexes with the organotin(IV) ions.

According to these considerations, the syntheses of the complexes, already described in [20], were somewhat modified (Scheme 2). The complexes were prepared by dissolving the appropriate amount of ligands (6 mmol of HL^1–HL^3 and HL^6, and 3 mmol of H$_2$L^4–H$_2$L^5 H$_2$L^7 and H$_2$L^8–H$_2$L^{11}) in dry MeOH (50 cm^3) and adding equimolar amounts of NaOH solution to each methanolic solution. After stirring and refluxing for 3 h, to this colourless solution a methanolic solution (50 cm^3)
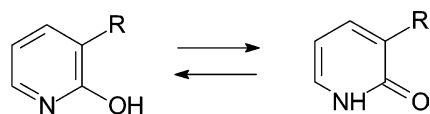
R = H for HL^1 and COOH for H$_2$L^{10}

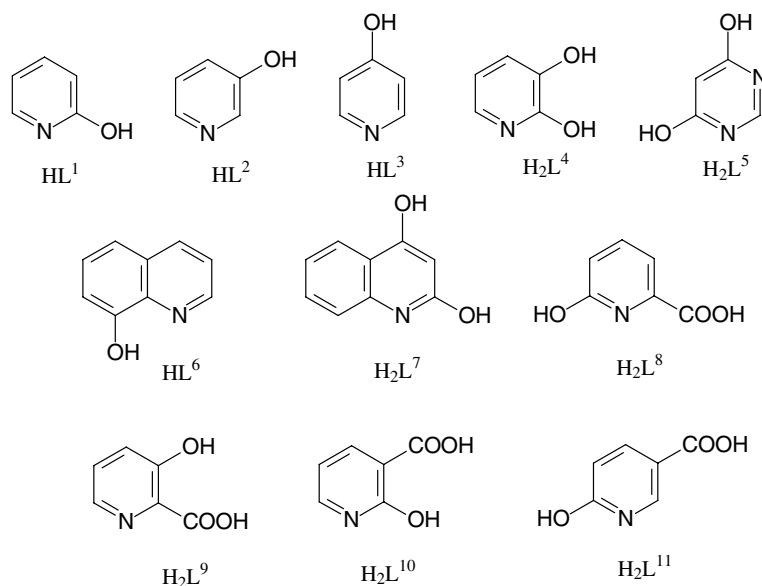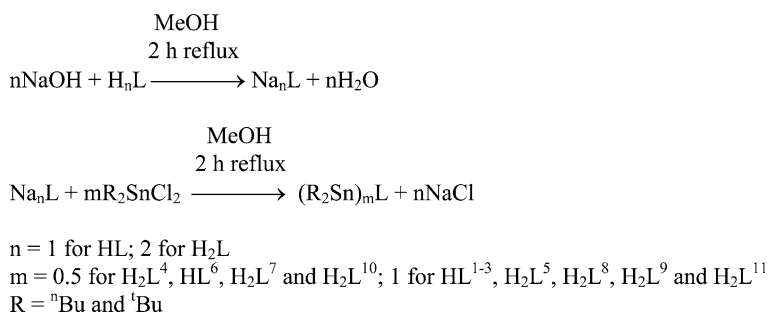Scheme 1. Enol–keto tautomerism of ligands HL^1 and H$_2$L^{10}.

Fig. 1. Structures of the ligands studied.

$$nNaOH + H_nL \xrightarrow[\text{2 h reflux}]{\text{MeOH}} Na_nL + nH_2O$$

$$Na_nL + mR_2SnCl_2 \xrightarrow[\text{2 h reflux}]{\text{MeOH}} (R_2Sn)_mL + nNaCl$$

n = 1 for HL; 2 for H$_2$L
m = 0.5 for H$_2$L^4, HL^6, H$_2$L^7 and H$_2$L^{10}; 1 for HL$^{1-3}$, H$_2$L^5, H$_2$L^8, H$_2$L^9 and H$_2$L^{11}
R = ^{n}Bu and ^{t}Bu

Scheme 2. Preparation of the complexes.

of R$_2$SnCl$_2$ (3 mmol) was added, and the refluxing was continued for a further 2 h.

Compounds **1n**, **3n**, **4n**, **5n**, **9n**, **10n**, **1t**, **3t**, **5t** and **9t** precipitated immediately from the mixture, while compounds **7n**, **8n**, **4t**, **7t**, **8t** and **10t** were obtained only after removal of the solvent under reduced pressure by rotary evaporation (the letters **n** and **t** denote *n*- and *t*-butyltin(IV) compounds, respectively). All these complexes were recrystallized from MeOH. Compounds **2n**, **6n**, **11n**, **2t**, **6t** and **11t** were obtained via slow evaporation of the solvent at room temperature (in a crystallizing dish loosely covered with a filter paper), and separated by filtration and washed with dry MeOH. The complexes obtained were all insoluble in water and benzene. Complexes **1n**–**4n**, **6n**–**8n**, **11n**, **2t**, **6t**–**8t** and **11t** were soluble in CHCl$_3$, and complexes **5n**, **9n**, **10n**, **3t**–**5t**, **9t** and **10t** only in DMSO. Compounds **6n** and **6t** were obtained as single crystals; the others were amorphous solids.

The analytical data on the compounds are presented in Table 1, together with other characteristic physical constants. C, H, N microanalyses were performed at

the Department of Organic Chemistry, University of Szeged. The Sn contents were measured by inductively coupled plasma atomic emission spectrometry (ICP-AES) and found to correspond to the theoretically calculated values.

2.3. X-ray crystallography

Crystal data and refinement parameters are listed in Table 2. Intensity data were collected on an Enraf-Nonius CAD-4 diffractometer with graphite monochromated Mo Kα radiation ($\lambda = 0.71073$ Å), using the $\omega - 2\theta$ scan technique. Three standard reflections were monitored every hour; these remained constant within experimental error. The structures were solved by direct methods (SHELXS-97) and refined by full-matrix least-squares (SHELXL-97) [22]. All non-hydrogen atoms were refined anisotropically in F^2 mode. Hydrogen atom positions were generated from assumed geometries. The riding model was applied for the hydrogen atoms. In both structures, the relatively high residual

Table 1
Physical and analytical data on $[Bu_2Sn(IV)]^{2+}$ complexes studied

Complex	Analysis (%)				Colour	M.p. (°C)
	C	H	N	Sn		
$[^nBu_2Sn(2\text{-hpy})(OH)]_n$ (**1n**)	45.05 (45.35)	6.44 (6.68)	4.69 (4.07)	33.75 (34.50)	White	195–197
$[^tBu_2Sn(2\text{-hpy})(OH)]_n$ (**1t**)	45.07 (45.35)	6.24 (6.68)	5.13 (4.07)	33.56 (34.50)	White	>300
$[^nBu_2Sn(3\text{-hpy})(OH)]_n$ (**2n**)	44.78 (45.35)	7.02 (6.68)	4.54 (4.07)	33.81 (34.50)	Light-yellow	148–150
$[^tBu_2Sn(3\text{-hpy})(OH)]_n$ (**2t**)	44.92 (45.35)	5.86 (6.68)	3.96 (4.07)	33.47 (34.50)	White	>300
$[^nBu_2Sn(4\text{-hpy})(OH)]_n$ (**3n**)	44.21 (45.35)	6.35 (6.68)	4.48 (4.07)	33.96 (34.50)	White	176–178
$[^tBu_2Sn(4\text{-hpy})(OH)]_n$ (**3t**)	44.84 (45.35)	6.21 (6.68)	3.73 (4.07)	34.15 (34.50)	White	>300
$^nBu_2Sn(2,3\text{-dhpy})_2$ (**4n**)	47.16 (47.68)	5.42 (5.74)	5.73 (6.18)	25.80 (26.20)	Deep-brown	172
$^tBu_2Sn(2,3\text{-dhpy})_2$ (**4t**)	47.46 (47.68)	5.16 (5.74)	6.36 (6.18)	26.46 (26.20)	Brown	234–236
$[^nBu_2Sn(4,6\text{-dhpym})]_n$ (**5n**)	42.47 (41.98)	6.83 (6.41)	8.53 (8.16)	33.97 (34.60)	Light-yellow	>300
$[^tBu_2Sn(4,6\text{-dhpym})]_n$ (**5t**)	41.72 (41.98)	6.25 (6.41)	8.32 (8.16)	34.23 (34.60)	Yellow	>300
$^nBu_2Sn(8\text{-hq})_2$ (**6n**)	59.63 (59.88)	5.47 (5.76)	5.08 (5.37)	22.50 (22.78)	Yellow	146–148
$^tBu_2Sn(8\text{-hq})_2$ (**6t**)	59.74 (59.88)	5.36 (5.76)	5.21 (5.37)	22.34 (22.78)	Colourless	202
$[^nBu_2Sn(2,4\text{-dhq})_2(H_2O)]$ (**7n**)	54.18 (54.64)	5.62 (5.95)	4.72 (4.90)	20.32 (20.84)	Light-brown	224–225
$^tBu_2Sn(2,4\text{-dhq})_2$ (**7t**)	56.23 (56.42)	5.13 (5.42)	4.87 (5.06)	20.93 (21.46)	Light-brown	268–270
$[^nBu_2Sn(6\text{-hpica})(H_2O)]$ (**8n**)	43.04 (43.30)	5.35 (5.93)	3.42 (3.61)	29.93 (30.59)	Brown	>300
$^tBu_2Sn(6\text{-hpica})$ (**8t**)	45.21 (45.40)	5.19 (5.67)	3.15 (3.78)	31.58 (32.08)	Brown	>300
$[^nBu_2Sn(3\text{-hpica})(H_2O)]$ (**9n**)	43.07 (43.30)	5.75 (5.93)	3.18 (3.61)	29.32 (30.59)	White	156–158
$[^tBu_2Sn(3\text{-hpica})(H_2O)]$ (**9t**)	42.69 (43.30)	5.47 (5.93)	3.74 (3.61)	29.87 (30.59)	White	180–182
$^nBu_2Sn(2\text{-hnica})_2$ (**10n**)	46.74 (47.15)	4.86 (5.11)	5.17 (5.50)	22.82 (23.32)	White	221
$^tBu_2Sn(2\text{-hnica})_2$ (**10t**)	47.42 (47.15)	5.34 (5.11)	5.78 (5.50)	23.27 (23.32)	White	249–251
$[^nBu_2Sn(6\text{-hnica})]_n$ (**11n**)	44.86 (45.40)	5.08 (5.67)	3.26 (3.78)	31.17 (32.08)	White	>300
$[^tBu_2Sn(6\text{-hnica})]_n$ (**11t**)	45.78 (45.40)	5.60 (5.67)	3.74 (3.78)	31.94 (32.08)	White	>300

Table 2
Summary of X-ray diffraction data for **6t** and **6n**

	6t	6n
Empirical formula	$C_{26}H_{30}N_2O_2Sn$	$C_{26}H_{30}N_2O_2Sn$
Formula mass	521.21	521.21
Crystal size (mm)	$0.30 \times 0.50 \times 0.60$	$0.35 \times 0.45 \times 0.60$
Colour	Colourless	Yellow
Crystal system	Monoclinic	Monoclinic
Space group	$C2/c$	$P2_1/c$
θ range for data collection (°)	$2.31 \leqslant \theta \leqslant 34.96$	$2.42 \leqslant \theta \leqslant 25.96$
a (Å)	13.990(1)	13.443(1)
b (Å)	9.780(1)	12.899(1)
c (Å)	18.278(1)	14.652(1)
β (°)	104.91(1)	104.84(1)
V (Å³)	2419.9(3)	2455.9(4)
Z	4	4
d_{calc} (Mg/m³)	1.432	1.410
μ (mm⁻¹)	1.081	1.064
$F(000)$	1064	1064
Index ranges (°)	$-22 \leqslant h \leqslant 22$	$-16h \leqslant 16$
	$-15 \leqslant k \leqslant 15$	$-7 \leqslant k \leqslant 15$
	$-29 \leqslant l \leqslant 29$	$0 \leqslant l \leqslant 18$
No. of reflections collected	11,760	5111
No. of independent reflections/R_{int}	5314/0.0145	4774/0.0187
No. of observed reflections $I > 2\sigma(I)$	4448	2475
No. of parameters	147	273
GOOF	1.097	0.908
R_1 (obsd. data)	0.0272	0.0515
wR_2 (all data)	0.0741	0.1532
Largest diff. peak/ hole (e Å⁻³)	0.537/−0.902	0.828/−0.502

electron density peaks of 0.537 (**6t**) and 0.828 (**6n**) e Å⁻³ lie ca. 0.74 (**6t**) and 0.98 Å (**6n**) from the high-electron scattering Sn atom. Cystallographic data (excluding structure factors) for the structures reported in this pa-

per have been deposited with the Cambridge Crystallographic Data Centre as Supplementary Publication Nos. CCDC-250424 (**6n**) and CCDC-250425 (**6t**). Copies of the data can be obtained free of charge on

Table 3
Partial quadrupole splitting (pqs) values of the functional groups used in the calculations (in mm s^{-1})

	T_d	TBP_a	TBP_e	O_h
{R}	− 1.37	−0.94	−1.13	−1.03
{COO$^-$}$_m$	−0.15	−0.1	0.06	−0.11
{COO$^-$}$_b$	0.114	0.075	0.293	0.083
{–C=O}	0.24	0.16	0.407	0.177
{N$_{pyridine}$}	−0.46	−0.035	0.147	−0.1
{N$_{heterocycle}$}	−0.46	−0.035	0.147	−0.1
{OH}	−0.40	−0.13	0.02	−0.14
{O$^-$}	−0.37	−0.21	−0.09	−0.27
{H$_2$O}	–	0.18	0.43	0.2

Abbreviations: T_d: tetrahedral, TBP_a: trigonal-bipyramidal axial, TBP_e: trigonal-bipyramidal equatorial, O_h: octahedral, m: monodentate, b: bidentate.

application to CCDC, 12 Union Road, Cambridge CB2 1EZ, UK [Fax: int. code +44(1223)336 033; e-mail: deposit@ccdc.cam.ac.uk].

2.4. FT-IR and Mössbauer spectroscopic measurements

The FT-IR spectra of the ligands and of the complexes were measured in KBr pellets on a BioRad Digilab Division FTS-65A instrument in the range 4400–400 cm^{-1}.

Mössbauer spectroscopic measurements were performed as described previously [19]. In order to determine the steric arrangement of the coordination sphere, the experimental quadrupole splitting values (Δ_{exp}) were compared with those calculated ($|\Delta_{calc}|$) for different possible tetra-, penta- and hexacoordinated symmetries of the Sn(IV) centres, according to point charge model formalism (partial quadrupole splitting (pqs) concept) [23]. On the basis of these calculations, the most probable stereochemistry of a given complex can be suggested. The pqs values of the different functional groups in question were taken in part from the relevant literature [24,25] (Table 3).

3. Results and discussion

3.1. X-ray structural studies

A search of the Cambridge Structural Database [26] reveals that the structure of 6n has been previously reported [27], however the refinement of the structure was incomplete since no hydrogen atoms were located. The results of the redetermination (Table 4) agree in all respects with those reported [27], but with improved precision since the hydrogen atoms are also included. In both 6n (Fig. 2) and 6t (Fig. 3), the tin centre is hexacoordinated in *cis*-O_h coordination geometry, with angles of 113.4(1)° (6t) and 111.2(3)° (6n) C–Sn–C, respectively. The quinolin-8-olato-*N,O* anion is bound to the

Table 4
Selected interatomic bond distances (Å) and bond angles (°) for complexes 6t and 6n

| 6t		6n	
Sn(1)–O(1B)	2.1229	Sn(1)–O(1B)	2.115(4)
		Sn(1)–O(1D)	2.088(3)
Sn(1)–N(1B)	2.3787	Sn(1)–N(1B)	2.359(5)
		Sn(1)–N(1D)	2.338(3)
Sn(1)–C(1A)	2.213(2)	Sn(1)–C(1A)	2.162(7)
		Sn(1)–C(1C)	2.158(7)
C(1A)–Sn(1)–C(1A)^i	113.4(1)	C(1C)–Sn(1)–C(1A)	111.2(3)
O(1B)–Sn(1)–N(1B)	72.7(1)	O(1B)–Sn(1)–N(1B)	73.2(2)
		O(1D)–Sn(1)–N(1D)	74.3(1)
O(1B)–Sn(1)–O(1B)^i	157.9(1)	O(1D)–Sn(1)–O(1B)	152.7(1)
O(1B)–Sn(1)–N(1B)^i	89.1(1)	O(1D)–Sn(1)–N(1B)	85.0(1)
		O(1B)–Sn(1)–N(1D)	84.9(1)
O(1B)–Sn(1)–C(1A)	89.8(1)	O(1B)–Sn(1)–C(1A)	91.4(3)
		O(1D)–Sn(1)–C(1C)	94.0(2)
C(1A)–Sn(1)–N(1B)^i	89.7(1)	C(1A)–Sn(1)–N(1D)	88.1(2)
		C(1C)–Sn(1)–N(1B)	85.3(2)
C(1A)–Sn(1)–N(1B)	153.8(1)	C(1A)–Sn(1)–N(1B)	159.4(3)
		C(1C)–Sn(1)–N(1D)	159.8(2)
N(1B)–Sn(1)–N(1B)^i	70.9	N(1B)–Sn(1)–N(1B)	77.3(1)

Symmetry code: (i) = −x, y, 1/2 − z.
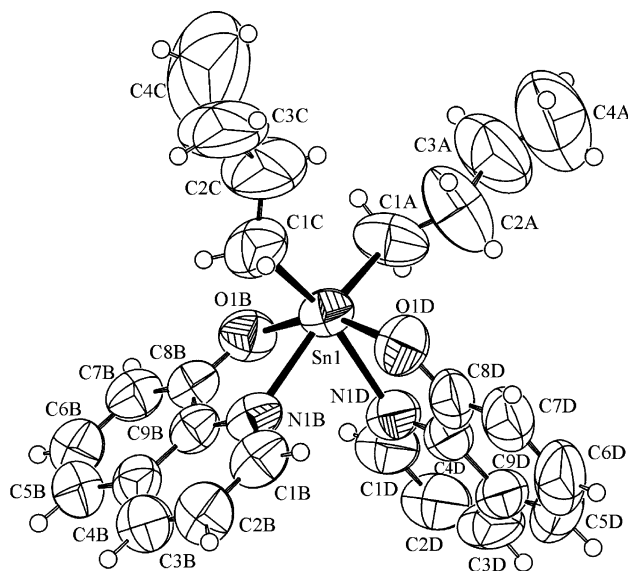
Fig. 2. A view of the molecular structure of ^{n}Bu$_2$Sn(8-hq)$_2$ (6n) showing the atom-numbering scheme. Non-hydrogen atoms are shown as 50% probability ellipsoids and hydrogen atoms are shown as open cycles.

metal centres in a bidentate chelating fashion, forming a five-membered SnONC$_2$ ring with an O–Sn–N bite angle of 72.7(1)° (6t), or of 73.2(2)° and 74.3(1)° (6n) (Table 4). In 6t, the O–Sn–O angle is ca. 5° greater than that for 6n, while the C–Sn–N angle of 153.8(1)° in 6t is smaller by ca. 6° than the corresponding angle in 6n (Table 4). In 6t, the π electrons of the five-membered chelate rings interact with the hydrogen of the *t*-butylic C(2A) to form weak C–H···π bonds (Table 5). In the same way, there are some potential C–H···π interactions
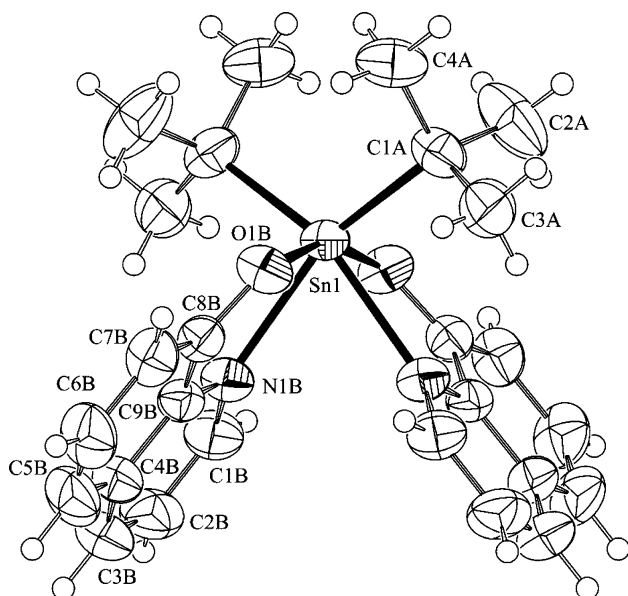
Fig. 3. A view of the molecular structure of $^tBu_2Sn(8-hq)_2$ (6t) showing the atom-numbering scheme. Non-hydrogen atoms are shown as 50% probability ellipsoids and hydrogen atoms are shown as open cycles.

(Table 5) in the crystal lattice of **6n**. These interactions should be regarded with some reservation since their geometric parameters are less accurate due to a relatively low quality of the crystal structure (partial disorder). The Sn–O and Sn–N bond distances of **6t** are almost equal as those of **6n**. It was interesting to observe that these complexes show no tendency to dimerize into heptacoordinated species via stannoxanic Sn–O bonds, as is common for both $^nBu_2Sn(O,O,N$-chelate) and $Me_2Sn(O,O,N$-chelate) complexes [19]. In the crystal lattices of **6t** and **6n**, additional C–H$\cdots\pi$ interactions are present (Table 5).

3.2. FT-IR spectroscopic characterization

The characteristic FT-IR bands observed and the vibrational assignments are detailed in Tables 6 and 7.

Table 5
Selected interatomic distances (Å) and angles (°) for the C–H$\cdots\pi$ interactions in **6t** and **6n** [a] Cg1, Cg2, Cg3 and Cg4 are the centroids of rings Sn1/O1B/C8B/C9B/N1B (chelate), C4B/ C5B/C6B/C7B/C8B/ C9B, Sn1/O1D/C8D/C9D/N1D (chelate) and N1B/C1B/ C2B/C3B/ C4B/C9B, respectively

Compound	D–H$\cdots$A	H$\cdots$A (Å)	D$\cdots$A (Å)	D–H$\cdots$A (°)
6t	C(2A)–H(2A)$\cdots$Cg1[a]	2.78	3.29	114
	C(3A)–H(3A)$\cdots$Cg2[b]	3.19	4.11	166
6n	C(2A)–H(1A)$\cdots$Cg3	3.00	3.42	107
	C(1D)–H(1D)$\cdots$Cg4[c]	3.13	3.75	126
	C(3D)–H(3D)$\cdots$Cg4[d]	2.71	3.56	153

[a] Symmetry codes: (a) $-x, y, 1/2 - z$; (b) $1/2 - x$, $1/2 + y$, $1/2 - z$; (c) x, $3/2 - y$, $-1/2 + z$; (d) $-x$, $1 - y$, $-z$.

Some hydroxypyridines, hydroxypyrimidines and hydroxyoxyquinolines are known [28] to exist in different forms (hydroxy-ketone). In the solid state, 2- and 4-hydroxypyridine are predominantly in pyridone form. In the spectra of free HL^1, HL^3, H_2L^4 and H_2L^7, there are characteristic medium and strong bands of the NH and C=O groups in the spectral regions 3210–3090 and 1650–1630 cm^{-1}. The spectra also support the existence of the keto form of H_2L^5 as $vC=O$ bands appear at 1680 and 1642 cm^{-1} (Table 6). In the cases of HL^2 and HL^6, these bands are absent from the spectra. This is because the tendency of tautomerization to their keto forms is small. The broad vOH absorption band in the region 3400–3200 cm^{-1} arises from the strong intra- and intermolecular hydrogen-bonding network of the free ligands.

Hydroxypyridine-carboxylic acids can also undergo tautomerization reactions. In the IR spectra of the free ligands H_2L^8, H_2L^{10} and H_2L^{11}, the bands corresponding to the OH group vibrations seem to be absent. The vOH (ca. 3400 cm^{-1}) [29] and the strong band at 1000 cm^{-1}, indicative of the pyridine structure [30], are not seen in the vibrational spectra. These features suggest that the ligands could possibly be in the keto rather than in the hydroxy form. Furthermore, the presence of the stretching vibrations $vC=O$ in the region 1740–1700 cm^{-1} and vNH in the region 3240–3200 cm^{-1}, and the in-plane βNH band at ca. 1607 cm^{-1} in the IR spectra of the free ligands (Table 7) suggest that the keto form predominates in the solid state [29]. In the case of H_2L^9, the basic pyridine {N} atom is not protonated, and therefore the typical vNH band at 3220 cm^{-1} is not present.

In the spectra of the complexes **1n–3n**, **5n**, **1t–3t** and **5t** the medium and strong bands of the –NH and –C=O groups characteristic of the keto tautomer have disappeared, due to the deprotonation of the ligands and the binding of the phenolate oxygen(s) to the metal ion. In the spectra of **1n–3n** and **1t–3t**, the presence of a weak new band at ca. 3667 cm^{-1}, attributed to the $v(Sn-)$ OH vibration mode, suggests that these complexes contain coordinated hydroxide ion.

The derivatives of 2-picolinic acid can be bound to the metal centres in a bidentate chelating manner, forming a five-membered $SnONC_2$ ring [20]. This is not possible for the nicotinic acid complexes. Characteristic variations are observed in the region of the absorption bands of the –COO$^-$ groups in the IR spectra of **8n**–**11n** and **8t–11t**. Ligands L^8 and L^9 exist in zwitterionic form, similarly to the common amino acids. The $v_{as}COO^-$ and v_sCOO^- stretching bands in their spectra can therefore easily be assigned (Table 7). For all the diorganotin(IV) complexes of the eight carboxylic acids studied, the separation between these two bands (the Δv value) indicates the monodentate coordination mode of the –COO$^-$ group ($\Delta v \sim 250–310$ cm^{-1}) (Table 7). In

Table 6
Assignment of characteristic FT-IR vibrations (cm^{-1}) of hydroxypyridines, hydroxypyrimidine and hydroxyoxyquinolines and their diorganotin(IV) complexes

Compounds	vOH	vNH	vC=O	$v_{a,s}$ C=C/N=C	vC–O	vC–O(Sn)	vSn–C	vSn–O
L^1	–	3150 m	1683 m 1649 vs	1608 s, 1575 s, 1539 s, 1455 m	1241 m	–	–	–
1n	3660 w	–	–	1602 w, 1539 m, 1513 m, 1418 m	–	1155 m	599 m, 534 m	454 w 406 m
1t	3666 w	–	–	1600 w, 1564 m, 1530 m, 1436 w	–	1166 s	594 m, 527 w	450w 411 w
L^2	3424 w	–	–	1574 vs, 1540 sh, 1479 vs, 1445 sh	1242 vs	–	–	–
2n	3660 w	–	–	1573 m, 1559 m, 1477 s, 1409 m	–	1182 w	597 m, 509 m	415 m
2t	3667 w	–	–	1563 s, 1547 m, 1470 s, 1420 s	–	1166 s	595 m, 522 w	405 w
L^3	–	3205 m	1670 sh, 1633 vs	1548 s, 1507 vs, 1428 msh	1190 vs	–	–	–
3n	3658 w	–	–	1543 m, 1520 m, 1474 sh, 1420 m	–	1155 w	607 m, 533 m	406 m
3t	3667 w	–	–	1563 brm, 1487 w 1425 w	–	1166 m	597 m, 520 m	406 m
L^4	3270 m	3240 m	1676 s, 1664 vs	1613 m, 1579 m, 1446 w, 1412 w	1189 s	–	–	–
4n	–	3245 w	1620 m	1606 s, 1540 vs, 1454 m, 1416 m	1188 m	1152 w	610 w, 588 w	462 w
4t	–	3240 m	1664 s	1609 vs, 1579 m, 1555 m, 1457 w	1189 s	1161 m	611 m, 575 w	445 w
L^5	–	–	1681 m, 1642 s	1607 vs, 1585 s, 1521 m, 1445 m	1234 s	–	–	–
5n	3420 w	–	–	1610 sh, 1580 vs, 1512 m, 1420 m	–	1242 s	548 m, 521 w	472 w
5t	3421 w	–	–	1605 vs, 1592 vs, 1487 m, 1420 m	–	1262 s	552 w, 512 w	470 w
L^6	3470 w	–	–	1580 m, 1509 vs, 1473 s, 1434 m	1208 m	–	–	–
6n	–	–	–	1571 m, 1497 s, 1464 vs, 1424 w	–	1109 s	614 w, 516 w	493 w
6t	–	–	–	1573 m, 1499 vs, 1465 vs, 1428 w	–	1108 s	612 m, 512 w	493 w
L^7	3380 w	3093 m	1689 vs	1610 s, 1594 vs, 1551 w, 1505 m, 1471 s, 1420 s	1234 vs	–	–	–
11n	3445 m	3092 m	1668 m	1595 vs, 1550 sh, 1494 m, 1458 s, 1420 m	1231 s	1155 w	554 m, 506 w	458 w
11t	–	3090 w	1674 m	1631 s, 1593 s, 1552 w, 1505 m, 1473 m, 1415 m	1235 s	1165 s	593 m, 508 w	456 w

Abbreviations: s: strong; m: medium; w: weak; vs: very strong, sh: shoulder.

Table 7
Assignment of characteristic FT-IR vibrations (cm^{-1}) of hydroxycarboxylic acids and their diorganotin(IV) complexes

Comp.	vOH	vNH	vC=O	v_aCOO$^-$	v_sCOO$^-$	Δv	$v_{a,s}$C=C/N=C	vSn–C	vSn–O
L^8	3415 w	3208 w	1715 s	1636 vs	1434 m	202	1600 m, 1538 m, 1434 m	–	–
8n	3430 w	–	–	1677 s	1404 m	273	1611 s, 1542 w, 1498 vs	618 w, 548w	492 w 443 w
8t	–	–	–	1633 vs	1357 m	276	1607 s, 1550 w, 1444 w	581 w, 542 w	451 w 415 w
L^9	3429 w	3220 sh	1702 m	1524 vs	1355 m	169	1609 m, 1555 sh, 1469 s, 1427 w	–	–
9n	3460 w	–	–	1597 vs	1336 m	261	1569 s, 1550 m, 1453 m, 1420 w	567 w	479 w
9t	3432 w	–	–	1595 vs	1339 m	256	1567 s, 1547 m, 1454 m, 1417 w	567 w	460 w
L^{10}	3431 w	3229 w	1743 s 1706 s	–	–	–	1607 m, 1550 m, 1486 m, 1448 m	–	–
10n	–	–	1730 sh	1612 vs	1339 m	273	1559 m, 1542 m, 1452 m, 1417 m	588 w	427 w 405 w
10t	–	3197 w	1740 sh	1651 vs	1358 m	293	1601 s, 1577 m, 1550 m, 1425 w	605 w, 520 w	430 w 407 w
L^{11}	3403 w	3232 w	1707 m 1650 vs	–	–	–	1607 vs, 1551 m 1471 w, 1430 m	–	–
11n	–	–	–	1623 s	1314 s	309	1594 vs, 1545 sh 1482 m, 1425 w	557 m, 519 w	426 w
11t	–	–	–	1634 s	1330 m	304	1606 vs, 1552 s 1494 w, 1413 m	585 w, 534 w	429 w

Abbreviations: s: strong; m: medium; w: weak; vs: very strong, sh: shoulder.

the spectra of **8n**, **9n**, and **9t**, the presence of the vOH stretch suggests that the compounds contain a coordinated H$_2$O molecule. For **10n** and **10t**, the presence of vNH and vC=O bands together with vCOO$^-$ bands confirms that the ligand coordinates in the pyridone form, with the formation of a six-membered chelate ring, involving the –COO$^-$ group and the {O} in position 2. The absence of vNH and vC=O bands from the spectra of **8n**, **8t**, **9n**, **9t**, **11n** and **11t** points to the tridentate coordination of these three ligands (Table 7).

As regards the coordination of the aromatic nitrogen, {N}, the behaviour of the vC=N/C=C bands is the most relevant (Tables 6 and 7). For **1n**–**3n**, **5n**, **6n**, **8n**, **9n**, **11n**, **1t**–**3t**, **5t**, **6t**, **8t**, **9t** and **11t**, the vC=N/C=C bands are shifted considerably towards lower frequencies with respect to the positions for the free ligands, confirming the coordination of the heterocyclic {N} to the diorganotin(IV) moiety. The stretching frequency is lowered owing to the transfer of electron density from {N} to the {Sn} atom. This results in weakening of the C=N bond as reported in the literature [31].

The bands assignable to the vC–O stretching vibration of the free ligands in the region 1300–1190 cm^{-1} are shifted by about 10–50 cm^{-1} upon complexation,

indicating the formation of a (C–)O–Sn bond. The shift indicates charge withdrawal from the C–O to the Sn–O bond(s), which is consistent with Sn–O covalent bonds.

The IR spectra of **6n** and **6t** are quite similar, suggesting that the structures of these compounds are very similar. The vibrational frequencies assigned to **6n** and **6t** correspond to the data reported for the complexes RSn(8-hq)$_3$ (8-hq = 8-hydroxyquinoline) [13]. Taking into account the correspondence of the IR spectra of the compounds, it may be concluded that the 8-hq ligands chelate to Sn(IV) through coordination by {O,N} atoms, in accordance with the results of X-ray diffraction structural analysis.

The presence of two (antisymmetric and symmetric) Sn–C absorption bands between 610 and 500 cm^{-1} in the spectra of all the compounds (except **9n**, **9t** and

10n) strongly suggests that the C–Sn–C bond angle is less than 180° [32]. This is in accord with the ^{119}Sn Mössbauer results.

3.3. Mössbauer spectroscopic characterization

In order to gain further structural information on the solid complexes, the Mössbauer spectra of the compounds were recorded and analysed. As examples, two typical Mössbauer spectra are depicted in Fig. 4. The ^{119}Sn Mössbauer spectroscopic parameters are listed in Table 8, together with the suggested configurations according to the pqs concept (Fig. 5) and the C–Sn–C bond angle of the compounds. The magnitudes of the isomer shift (δ) indicate an oxidation state of Sn(IV) for all the complexes.
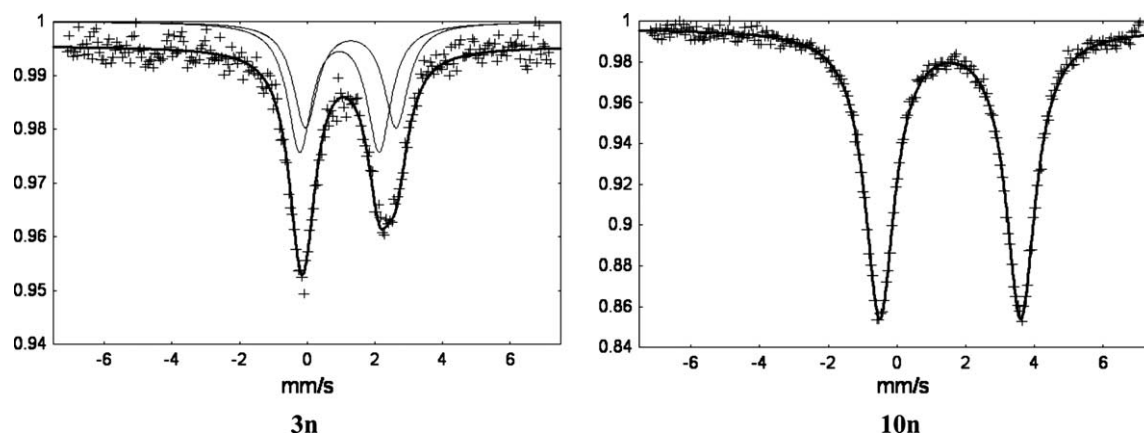

Fig. 4. Experimental Mössbauer spectra of **3n** and **10n**.

Table 8
Experimental and calculated Mössbauer spectroscopic parameters of complexes

Complex	δ_1	$|\Delta|_{1e}$	$|\Delta|_{1c}$	Γ_1	δ_2	$|\Delta|_{2e}$	$|\Delta|_{2c}$	Γ_2	Geom. 1	Geom. 2	Θ_1	Θ_2
1n	1.38	2.71	2.71	0.85	0.93	2.53	2.65	0.97	TBP1	TBP2	120	114
1t	1.31	2.68	2.71	1.27	–	–	–	–	TBP1	–	119	–
2n	1.35	2.68	2.71	0.90	0.97	2.45	2.65	0.90	TBP1	TBP2	119	112
2t	1.27	2.54	2.65	1,02	–	–	–	–	TBP2	–	114	–
3n	1.32	2.78	2.71	0.94	0.95	2.39	2.65	0.97	TBP1	TBP2	122	112
3t	1.26	2.30	2.65	1.14	–	–	–	–	TBP2	–	107	–
4n	1.46	3.36	3.31	1.00	0.89	2.72	2.85	1.00	O$_h$1	TBP3	138	120
4t	1.22	3.24	3.31	1.06	–	–	–	–	O$_h$1	–	134	–
5n	1.24	3.02	2.70	0.99	–	–	–	–	O$_h$2	–	128	–
5t	1.34	2.80	2.70	0.97	–	–	–	–	O$_h$2	–	122	–
6n	0.94	2.10	2.04	0.90	–	–	–	–	O$_h$3	–	96	–
6t	1.14	2.10	2.04	0.93	–	–	–	–	O$_h$3	–	96	–
7n	1.21	3.32	3.12	0.98	–	–	–	–	TBP6	–	137	–
7t	1.25	2.56	2.31	0.88	–	–	–	–	T$_d$1	–	116	–
8n	1.45	3.90	3.92	0.92	–	–	–	–	O$_h$5	–	158	–
8t	1.62	3.12	3.22	0.84	1.35	2.83	2.80	0.91	TBP4	TBP5	131	123
9n	1.37	3.77	3.91	0.91	–	–	–	–	O$_h$6	–	152	–
9t	1.58	3.70	3.91	0.98	–	–	–	–	O$_h$6	–	150	–
10n	1.55	4.10	4.25	1.04	–	–	–	–	O$_h$7	–	173	–
10t	1.57	3.58	3.73	1.04	–	–	–	–	O$_h$7	–	144	–
11n	1.26	3.10	3.22	0.96	–	–	–	–	TBP4	–	130	–
11t	1.62	3.24	3.22	0.91	–	–	–	–	TBP4	–	134	–

δ, $|\Delta|$ and Γ are given in mm s^{-1}, TBP: trigonal-bipyramidal, O$_h$: octahedral, Θ_1 and Θ_2 are C–Sn–C bond angles, given in degrees.

The full-width at half-maximum of the peaks (Γ) and the asymmetrical shape of the Mössbauer spectra of the $^nBu_2Sn(IV)^{2+}$ compounds **1n**–**4n** indicate more than one environment for these compounds. Resolution of the spectra of **1n**–**3n** results in adjacent quadrupole splitting values ($\Delta_{exp1} - \Delta_{exp2} = 2.39$–$2.78$ mm s^{-1}), in which both of the suggested stereochemistry forms are TBP (TBP1 and TBP2), differing only in the relative positions of the phenolate and hydroxy groups. In contrast with these spectra, the ^{119}Sn Mössbauer spectra of the analogous $^tBu_2Sn(IV)$ compounds (**1t**–**3t**) exhibit only a symmetrical doublet. In these $^tBu_2Sn(IV)$ complexes, the bulkiness of the t-butyl groups prevents the formation of two isomers, allowing the formation of only one Sn environment. These ligands are coordinated in bidentate {N,O} fashion to the $R_2Sn(IV)^{2+}$ centre. Complexes **1n** and **1t** can be monomers containing four-membered planar metallocycles (Sn–N–C–O) in a TBP environment (Fig. 6(a)), similarly to the diorganotin(IV) complexes

of 2-mercaptopyridine [33]. Complexes **2n**, **2t** and **3n**, **3t**, however, form only long-chain polymers with $R_2Sn(IV)^{2+}$ (Fig. 6(b)).

In the cases of H_2L^4 and H_2L^7, the analytical and IR data suggest the formation of protonated complexes $M(HL)_2$. The pqs calculations suggested that in **4n** the Sn(IV) centres are in O_h and TBP environments. The Δ_{exp} values of these two complexes indicate that the structure of **4t** is the same as in **4n** (O_h1), with the two alkyl groups in *cis* positions.

The FT-IR measurements revealed the disappearance of the NH and C=O bands characteristic of the keto tautomer. This is indicative of the deprotonation and bidentate coordination of the ligand. Moreover, both the m.p. data and the low solubility of **5n**, **5t**, **11n** and **11t** suggest a long-chain or ring-forming oligomeric structure of these compounds. In such complexes, the oligomerization proceeds through two pairs of phenolate O and neighbouring N donor atoms, where the
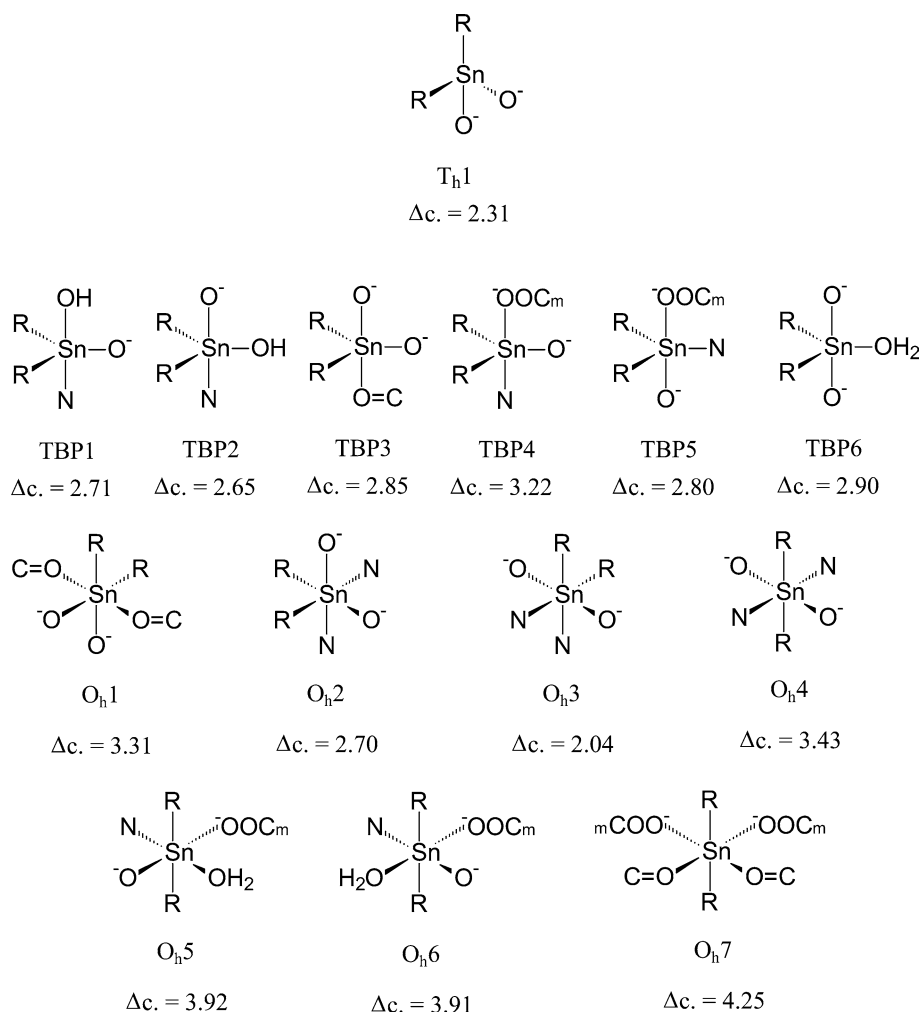

Fig. 5. Calculated quadrupole splitting values for the Sn(IV) coordination spheres in different stereochemical arrangements. m: monodentate coordination mode.
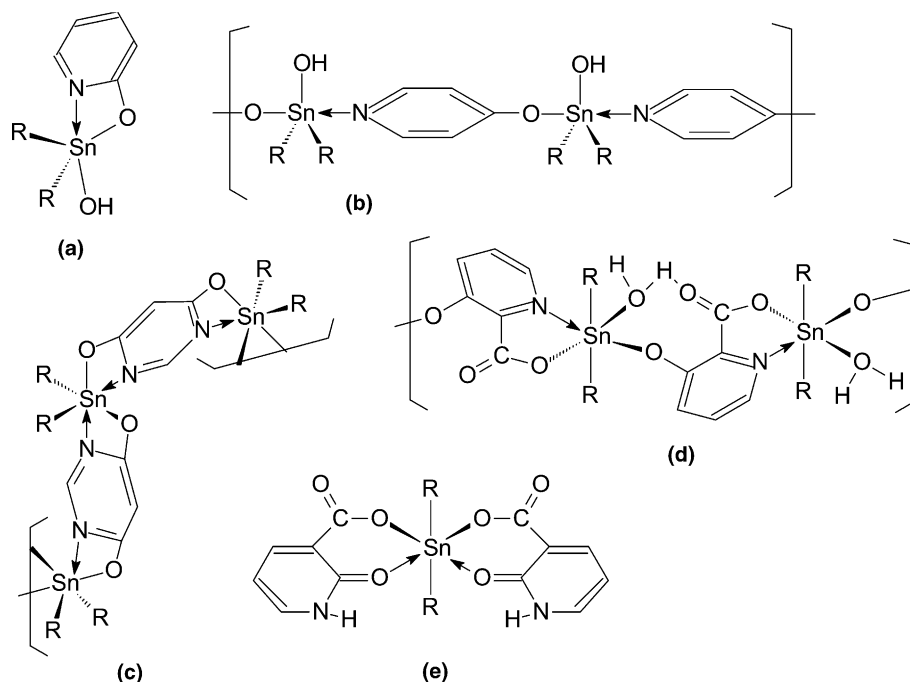
Fig. 6. Proposed structures for some selected complexes; R = *n*-Bu or *t*-Bu group; a – monomeric mixed hydroxo complex of **1**, b, c and d – repeating units of **3**, **4** and **9**, respectively, e – monomeric complex of **10**.

Sn(IV) centres are in similar distorted O_h environments, with the two alkyl groups in the *cis* position (Fig. 6c).

For **6n** and **6t**, it might be expected that these compounds will differ in structure in the same way as the $^nBu_2Sn(IV)$ and $^tBu_2Sn(IV)$ complexes of dipicolinic acid [19,20], but the X-ray diffraction results demonstrate the high conformity of the investigated compounds. This is in accordance with the measured and calculated Mössbauer parameters, which are exactly the same. The results of pqs calculations also reveal the formation of distorted *cis*-O_h structures, with the {N,O} chelation of Sn.

When the calculated Δ_{calc} values, based on different environments around the Sn(IV), were compared with the experimentally observed data for **7t**, reasonable agreement (2.31 mm s^{-1} in Table 8) was achieved with T_d. The coordination polyhedron includes the two deprotonated phenolate O donor atoms and the two alkyl groups (Fig. 5). The FT-IR spectrum of **7n** exhibits one intense νOH band, interpreted as due to the presence of a coordinated H_2O molecule. This means that coordination number of **7n** must be higher than four. We suggest a TBP configuration with the *n*-butyl groups and the H_2O in *eq* positions and the deprotonated phenolate oxygen donor atoms in *ax* positions.

The FT-IR spectroscopic measurements indicate only the monodentate coordination mode in **8n–11n** and **8t–11t**. Rationalization of the nuclear quadrupole splittings by using the pqs values, as in [20], showed that in the

majority of these complexes the central {Sn} atom is present in either a TBP or as O_h environment (Δ_{exp} = 3.60 ± 0.5 mm s^{-1}). In the suggested configurations (Fig. 5) there is no significant variation in the structures with the type of the alkyl group, except in **8n** and **8t**, where the ^nBu and ^tBu groups occupy *ax* and *eq* positions in O_h and TBP environments, respectively.

For H_2L^8 and H_2L^9, it is important to note that there is a –COO$^-$ group in the *ortho* position (relative to the ring {N} atom), which allows the formation of a stable five-membered chelate ring. Moreover, dimeric or oligomeric complexes can be formed (Fig. 6(d)), depending on the position of the –OH group. The identical Mössbauer parameters of **8n**, **9n** and **9t** suggest that the symmetry of the coordination sphere of the Sn(IV) does not depend on the steric situation of the hydroxy group on the carbon atoms in positions 6 and 3. It can be seen that the experimental |Δ_{exp}| values of these compounds are close to that calculated for two different (O_h5 and O_h6) stereochemistries.

The difference in the experimental Δ_{exp} values obtained for **10n** and **10t** can be interpreted in terms of the difference between the C–Sn–C angles (173° and 144°, see Table 8). In both compounds, 3-hydroxy-nicotinic acid coordinates via –COO$^-$ and C=O oxygen donor atoms in *eq* positions (Fig. 6(e)).

Compounds **11n** and **11t** may also be dimeric or very long chain-like, as are complexes **8n**, **8t**, **9n** and **9t**. Both alkyl groups are located in *eq* positions in the

TBP coordination sites. The oligomerization occurs through the monodentate $-COO^-$ group and the basic {N} and deprotonated phenolate {O} moieties of the different ligands (Fig. 5).

For Sn(IV) complexes containing a $R_2Sn(IV)$ moiety, the quadrupole splitting is dominated by highly covalent Sn–C bonds and, if the contributions of the other ligands are ignored, it can be shown that $|\Delta|$ is given [34] by

$$|\Delta| = -4[R][1 - (3/4)\sin^2\theta]^{1/2}, \tag{1}$$

where [R] denotes the pqs value of group R, and θ is the C–Sn–C angle. Eq. (1) has been satisfactorily applied to penta- and hexacoordinated Sn(IV) compounds, with the use of appropriate values of [R] for each coordination number [25]. The calculated θ angles are listed in Table 8. The nature of the R groups does not reveal any structural influence in the complexes studied, except for **7n**, **7t**, **8n** and **8t**. The experimental $|\Delta|$ values suggest a larger C–Sn–C angle for $^nBu_2Sn(IV)$ than for the $^tBu_2Sn(IV)$ complexes. This observation is in good agreement with the results obtained for the $^nBu_2Sn(IV)$ and $^tBu_2Sn(IV)$ complexes of pyridine mono- and dicarboxylic acids [19,20].

4. Conclusions

The synthetic procedures used in this work resulted in the formation of $^nBu_2Sn(IV)$ and $^tBuSn(IV)$ compounds with metal-to-ligand ratios of 1:1 and 1:2. The FT-IR and Mössbauer spectroscopic data for complexes **1–7** are indicative of penta- and hexacoordinated (i.e., TBP and O_h) geometries with the alkyl groups in the *eq* positions. In compounds **8n**, **9n**, **9t**, **10n** and **10t**, the presence of the carboxylate groups increases the C–Sn–C angle and the butyl groups move to *ax* positions. X-ray structural studies demonstrate the high conformity of **6n** and **6t**. In the polymeric compounds, the polymerization occurs through the different donor groups of the ligands, which bridge two central {Sn} atoms. Mössbauer spectroscopic measurements in combination with FT-IR spectroscopy allowed identification of the most probable steric arrangement around the Sn. The spectroscopic data are in agreement with the results of X-ray diffraction measurements.

Acknowledgements

References

[1] L. Pellerito, L. Nagy, Coord. Chem. Rev. 224 (2002) 111.
[2] Y. Nath, S. Pokharia, R. Yadav, Coord. Chem. Rev. 215 (2001) 99.
[3] C. Wei, N.W. Kong, V.G. Kumar Das, G.B. Jameson, R.J. Butcher, Acta Crystallogr. C 46 (1990) 2034.
[4] W. Chen, W.K. Ng, V.G. Kumar Das, G.B. Jameson, R.J. Butcher, Acta Crystallogr. C 45 (1989) 861.
[5] S.W. Ng, C. Wei, V.G. Kumar Das, J.P. Charland, F.E. Smith, J. Organomet. Chem. 364 (1989) 343.
[6] E. Kellö, V. Vrábel, J. Holeček, J. Sivy, J. Organomet. Chem. 493 (1995) 13.
[7] J.N.R. Ruddick, J.R. Sams, J. Chem. Soc., Dalton Trans. (1974) 470.
[8] T.K. Sham, G.M. Bancroft, Inorg. Chem. 14 (1975) 2281.
[9] S.N. Bhide, P. Umapaathy, M.P. Gupta, D.N. Sen, J. Inorg. Nucl. Chem. 40 (1978) 1003.
[10] V.G. Kumar Das, S.W. Ng, P.J. Smith, Inorg. Chim. Acta 49 (1981) 149.
[11] A. Lyčka, J. Holeček, A. Sebald, I. Tkac, J. Organomet. Chem. 409 (1991) 331.
[12] A. Lyčka, J. Holeček, M. Nadvornik, Main Group Metal Chem. 12 (1989) 169, and references therein.
[13] M. Schürmann, R. Schmiedgen, F. Huber, A. Silvestri, G. Ruisi, A.B. Paulsen, R. Barbieri, J. Organomet. Chem. 584 (1999) 103, and references therein.
[14] S. Wang, Polyhedron 17 (1998) 831.
[15] S. Maity, R. Roy, C. Sinha, W.-J. Sheen, K. Panneerselvam T.-H. Lu, J. Organomet. Chem. 650 (2002) 202.
[16] O. Castillo, A. Luque, F. Lloret, P. Roman, Inorg. Chim. Acta 324 (2001) 141.
[17] S. Gatto, T.I.A. Gerber, G. Bandolli, J. Perills, J.G.H. Preez, Inorg. Chim. Acta 269 (1998) 235.
[18] S.M.O. Quintal, H.I.S. Nugiera, V. Félix, M.G.B. Drew, Polyhedron 21 (2002) 2783.
[19] A. Szorcsik, L. Nagy, J. Sletten, G. Szalonati, E. Kamu, T. Fiore, L. Pellerito, E. Kálmán, J. Organomet. Chem. 689 (2004) 1145.
[20] A. Szorcsik, L. Nagy, A. Deák, M. Scopelliti, Z.A. Fekete, Á. Császár, C. Pellerito, L. Pellerito, J. Organomet. Chem. 689 (2004) 2762.
[21] P. Beak, Acc. Chem. Res. 10 (1977) 186.
[22] G.M. Sheldrick, SHELXS-97-Program for Crystal Structure Determination and SHELXL97-Program for the Refinement of Crystal Structures, Universität Göttingen, Germany, 1997.
[23] M.G. Clark, A.G. Maddock, R.H. Platt, J. Chem. Soc., Dalton Trans. (1972) 281.
[24] G.M. Bancroft, R.H. Platt, Adv. Inorg. Chem. Biochem. 15 (1972) 59.
[25] G.M. Bancroft, V.G. Kumar Das, T.K. Sham, M.G. Clark, J. Chem. Soc., Dalton Trans. (1976) 643.
[26] F.H. Allen, R. Taylor, Chem. Soc. Rev. 33 (2004) 463.
[27] D. Shi, S. Hu, Chin. J. Struct. Chem. 7 (1988) 111.
[28] H.I. Abdulla, M.F. El-Bermani, Spectrochim. Acta Part A 57 (2001) 2659.
[29] K. Nakamoto, Infrared and Raman Spectra of Inorganic and Coordination Compounds, Wiley, New York., 1997.
[30] K.M. Mukherjee, T.N. Misra, J. Raman Spectrosc. 27 (1996) 595.
[31] S.G. Teoh, G.Y. Yeap, C.C. Loh, L.W. Foong, S.B. Teo, H.K. Fun, Polyhedron 16 (1997) 2213, and references therein.
[32] H. Geissler, H. Kriegsmann, J. Organomet. Chem. 11 (1968) 85.
[33] R. Schmiedgen, F. Huber, H. Preut, G. Ruisi, R. Barbieri, Appl. Organomet. Chem. 8 (1994) 397, and references cited therein.
[34] R.V. Parish, Structure and bonding in tin compounds, in: G.J. Long (Ed.), Mössbauer Spectroscopy Applied to Inorganic Chemistry, Plenum Press, New York and London, 1984.